TU Delft

Delft University of Technology

Fatigue behaviour of a welded I-section under a line load in compression

Wardenier, Jaap; de Vries, Peter; Timmerman, Gerrit

DOI
10.1016/j.jcsr.2016.08.022

Publication date
2017

Document Version
Accepted author manuscript

Published in
Journal of Constructional Steel Research

Citation (APA)
Wardenier, J., de Vries, P., & Timmerman, G. (2017). Fatigue behaviour of a welded I-section under a line load in compression. *Journal of Constructional Steel Research*, *128*, 210-218. https://doi.org/10.1016/j.jcsr.2016.08.022

Important note
To cite this publication, please use the final published version (if applicable).
Please check the document version above.

Copyright
Other than for strictly personal use, it is not permitted to download, forward or distribute the text or part of it, without the consent of the author(s) and/or copyright holder(s), unless the work is under an open content license such as Creative Commons.

Takedown policy
Please contact us and provide details if you believe this document breaches copyrights.
We will remove access to the work immediately and investigate your claim.

This work is downloaded from Delft University of Technology.
For technical reasons the number of authors shown on this cover page is limited to a maximum of 10.

Journal of Constructional Steel Research

Title: Fatigue behaviour of a welded I-section under a line load in compression

Article Type: Research Paper

Key Words: Crane runway girder, compression load, fatigue, fatigue cracks, crack growth, residual tensile stresses.

Corresponding Author: Prof.dr.ir.Jaap Wardenier

Manuscript region: Netherlands

Abstract

This paper is part of an evaluation of fatigue cracks in a crane runway girder with full penetration welds between the web and flange. The fatigue analysis of this actual crane runway girder is described in [1].

The investigation described in this paper deals with additional experimental tests on equivalent welded I sections on scale of approximately 1:2 subjected to a fluctuating line load in compression. The objective of these experimental investigations is to investigate whether cracks stop or nearly stop when they have grown through the residual tensile stress field.

The test results show that, in some cases the cracks in the weld, at the weld toe with the web or with the flange initiate and grow from one side to about 50 to 60% of the web thickness and then stop. However, at the weld toe with the flange the cracks grow sometimes from both sides but with the cracks at one side having a small length and/or a small depth. The minimum ratio in life between crack initiation and maximum crack was a factor 1.2 for cracks occurring at one side only and 1.5 to 3.1 for cracks at both sides.

Research highlights

- The paper presents fatigue test results of a welded I beam under a compression line loading.
- The tests show that in most cases cracks initiate from one side and grow up to about 50 to 60% of the web thickness and then stop. In some cases they grow from both sides.
- Crack growth from one side is considerably faster than crack growth from both sides.
- The test results suggest that EN 1993-1-9 and EN 1993-6 for crane runway girders may be too conservative.

Fatigue behaviour of a welded I-section under a line load in compression

Jaap Wardenier*[a], Peter de Vries[b], Gerrit Timmerman[c]

[a] Wardenier & Associates, Delft University of Techn. and National University of Singapore

[b] Delft University of Technology, Delft

[c] PT Structural Design & Analysis B.V., Ridderkerk

*Corresponding Author; E-mail: j.wardenier@tudelft.nl

Abstract

This paper is part of an evaluation of fatigue cracks in a crane runway girder with full penetration welds between the web and flange. The fatigue analysis of this actual crane runway girder is described in [1].

The investigation described in this paper deals with additional experimental tests on equivalent welded I sections on scale of approximately 1:2 subjected to a fluctuating line load in compression. The objective of these experimental investigations is to investigate whether cracks stop or nearly stop when they have grown through the residual tensile stress field.

The test results show that, in some cases the cracks in the weld, at the weld toe with the web or with the flange initiate and grow from one side to about 50 to 60% of the web thickness and then stop. However, at the weld toe with the flange the cracks grow sometimes from both sides but with the cracks at one side having a small length and/or a small depth. The minimum ratio in life between crack initiation and maximum crack was a factor 1.2 for cracks occurring at one side only and 1.5 to 3.1 for cracks at both sides.

Key Words

Crane runway girder, compression load, fatigue, fatigue cracks, crack growth, residual tensile stresses.

1. Introduction

This paper is part of an evaluation of fatigue cracks in a crane runway girder with full penetration welds between the web and flange. After 20 years of service fatigue cracks were observed which were initiated at the transition of the toe of the full penetration weld with the flange. The observed cracks in the crane runway girder vary in length from a few mm to 330 mm with a summation of the lengths of all observed cracks being 750 mm, on a total length of 56 000 mm, thus being only 1.3%. The fatigue analysis of this actual crane runway girder is described in [1]. Although the external loading by the crane wheels is in compression, due to the residual tensile stresses in the outer layers of the welds the stress ranges at the critical notch locations at the weld toes are in tension, resulting in the observed fatigue cracks.

The research in this paper deals with additional experimental tests on equivalent welded I sections to investigate whether in multi-layered welds cracks stop or nearly stop when they have grown through the residual tensile stress field.

A test set-up with a rolling wheel with relatively high loading would result in a complicated test set-up with a low test frequency and consequently would be extremely expensive. That is why tests on a scale of approximately 1:2 have been carried out with a fixed wheel compression loading and with a line loading. Furthermore, smaller scaled test specimens would result in less weld layers and in considerably different residual stresses. This paper deals with the test results of the tests with a line loading

These results are compared with those which became recently available from the German AIF/Fosta research program [3, 4] by the University of Stuttgart. All other literature studied, only provides qualitative information but not evidence directly related to this subject.

1.1 Behaviour under a rolling wheel vs. that under a concentrated load and a line load

As extensively discussed by Kuhlmann et al. [3] and Euler and Kuhlmann in [4] and shown in Fig. 1, a rolling wheel on a crane runway girder produces for a particular location a normal

stress range $\Delta\sigma_z$ and an additional local shear stress range $\Delta\tau_{local}$. This results, for every wheel passing, in a shift of the direction of the principal stress. Therefore, Kuhlmann et al. [3] state that the summation of the individual damages for normal stresses and shear stresses as used in EN 1993-1-9 [5] and EN 1993-6 [6] is not appropriate for the non-proportional multi-axial loadings as occurring under a rolling wheel. They report [3] that their tests related to the normal stress range $\Delta\sigma_z$ only, based on the effective width given in EN 1993-6 [6] and ignoring the shear stress range, results in class 92 N/mm^2 at 2x10^6 cycles for welds with no full penetration.

Under a concentrated wheel loading the local shear stresses τ_{local} at both sides of the concentrated load are proportional to the normal stress range $\Delta\sigma_z$ but the maxima are not occurring at the same location. Further, the local shear stress range $\Delta\tau_{local}$ according to 1993-6 [6] will be equal to 0.2 $\Delta\sigma_z$ for a constant wheel load which is half of that under a rolling wheel. Since under a concentrated wheel loading the load is concentrated at one location and the cracks grow into a lower-stressed area, the crack growth in length direction will be slower than that under a rolling wheel, resulting in a better behaviour compared to that under a rolling wheel.

In case of a line load the stress σ_z is continuously perpendicular to the weld toe with the web. Although the induced shear stresses due to contraction at the weld toe with the flange will be different from that under a rolling wheel, the effect of the shear stresses is expected to be small, see [1]. If the normal stress σ_z under a rolling wheel is based on a representative effective width the class can be related to that of a detail with uniform loading which agrees with the philosophy used in [7].

2. Test specimens

The I-beam specimens shown in Fig. 2 are on scale of approximately 1:2 and were made in such a way that both the top side and the bottom side of a specimen could be used as a test location. The test specimens for the line loading tests had a length of 250 mm which was taken somewhat larger than the maximum crack lengths of 220 to 240 mm which occurred in the 8 concentrated wheel load tests.

Since the crane vessel [1] was built in the 80's, some steel types were no longer available. However, the steel types for the test specimen were selected in close cooperation with the steel suppliers to obtain steel characteristics (yield and tensile stresses) close to the original types, although the way of manufacturing could not be checked. The dimensions, steel grades and qualities of the line load test specimens are given in Table 1.

The welding procedure specification (SMAW process, electrodes, layers, preheating temperature) for the scaled full penetration welds of the web with the top and bottom flange was carefully specified. Since in the actual crane runway girder [1] prefabricated welded T sections are used for the flange and the upper part of the web, a horizontal down hand position is used for all welds. Welding distortions were limited during fabrication. Further, as in the actual crane runway girder, the flanges were machined flat from 40 mm to 35 mm. No afterward heat treatments of the welds and surrounding areas have been used after fabrication of the specimens. All specimens were carefully ultrasonically checked on defects which were not present. To allow better NDT inspection of the welds, a removable rail was provided on the top flange and to the bottom flange of the specimen. The ends of the specimens are without end plates and have been polished to avoid end effects on crack initiation.

For comparison with the results of the specimens with wheel loading, in each line load specimen one location (bottom side in the test rig) was provided at both sides of the web at the weld toe with the flange with an artificial defect whereas at the other location (top side in the test rig) had no artificial defects.

Note: The tests with artificial defects were incorporated for comparison with the wheel load tests [2] where the first two tests did not show cracking, even after $10x10^6$ cycles. These specimens were therefore provided with artificial defects and retested. The artificial elliptical shaped defects at both sides of the web were made by the electrical discharge machining method. The sharp edged artificial defects were 20 mm in length with a maximum depth of 2 mm, and 0.5 mm wide under an angle of 10º with the flange, see Fig.3. Based on the in-service inspections the angle of 10° was chosen.

3. Test Rig, Testing Procedure and Measurements

3.1 Test rig

The test rig, shown in Fig. 4, consists of 2 welded box section columns provided with holes and supporting blocks to allow heavy welded U beam sections to be fixed at the required levels. The jack applies a pushing force in upward direction.

As shown in Fig. 4 the specimens are loaded simultaneously at the top and at the bottom. At the location with artificial defects (bottom side in the test rig) the load was introduced by a straight loading block, at one side with the same cross section as the wheel. At the location without artificial defects (top side in the test rig) the load was introduced by a flat thick plate above the rail. The load range $-1.05\Delta F$ to $-0.05\Delta F$ was close to that in service, i.e.: $-\Delta F$ to 0.

3.2 Testing Procedure

Since the welds at both sides were not perfectly the same and the flange thickness also varied, positioning of the specimen and the loading block was generally carried out using auxiliary adjusting devices. This was done in such a way that the strains in the web at both sides at approximately $0.5t_w$, $0.8t_w$ and $1.5t_w$ from the web weld toe (with t_w = web thickness) were about the same, taking account of the exact location. Further tuning was performed by increasing the loads in steps and adjusting the wheel where required. In this way the

specimens were loaded at three pre-loading levels of approximately 1/3, 2/3 and 3/3 of the planned maximum compression load level. After this static tuning procedure, on each specimen three dynamic load tuning tests were carried out at a frequency of 0.1 Hz, 1 Hz and 3 Hz, each during about 20 cycles. After this tuning process the specimen was ready for testing.

3.3 Measurements

The following data were recorded:

- the actual dimensions of the welds at both sides (N and S) of the web, i.e. b_w and h_w in Fig. 5 (N = North and S = South).
- strains in the strain gauges for positioning in the test rig and for monitoring crack initiation and propagation.
- number of cycles at the visually observed crack length and NDT crack depth measurements.
- visually observed crack initiation and crack length measurements.
- number of cycles at end of crack propagation and end of test.

4. Testing program and test results

4.1 Tests without artificial defects

For the tests with line loads, shown in Tables 2 and 3, three tests have been carried out without artificial defects, i.e. 2LB and 4LA with a load range ΔF of 1522 kN and test 3LA with a load range of 1140 kN. The sides of the specimens are indicated as N and S, being North and South.

The "nominal" stress ranges $\Delta\sigma_i$ at the weld toe with the flange (5th column in Table 2) is the calculated average $\Delta\sigma_i = \Delta F/(lx(2b_w+t_w))$, where l and t_w are respectively the length of 250 mm of the specimen and the actual web thickness of the specimen and $2b_w$ is the sum of the fillet weld reinforcements at both weld toes with the flange. The stress range in the web (4th

and 5th column in Table 3) is determined in two ways, i.e. the average stress range $\Delta\sigma_i = \Delta F/(lxt_w)$ and that based on the measured governing strain range where the crack started; the latter with $E = 2.1x10^5$ N/mm^2 is used in the analysis.

4.1.1 Test 2LB

The governing S side for cracking had, a maximum measured $\Delta\sigma_i$ in the web of 174 N/mm^2. Crack initiation started at $0.9x10^6$ at both sides N and S. At the N side the crack remained in the weld and propagated to the weld toe of the flange but the crack stopped at $1.4x10^6$ cycles, see Fig. 6. At the N side the maximum crack depth, measured perpendicular to the web, was 6 mm.

At the S side, cracks initiated and grew from the weld toe of the flange, the weld and from the weld toe of the web, see Fig. 6. At $N = 1.4x10^6$ the maximum crack lengths were reached and at the edges no further crack growth in depth was observed. At the S side the maximum crack depths, both at the weld toe with the web and with the flange were 15 mm. Fig. 7 shows the most critical cross sections at the centre; this is one of the specimens with the most severe cracks. The test was stopped at $2.08x10^6$ cycles.

4.1.2 Test 3LA

At the weld toe with the web the governing N side had a maximum measured $\Delta\sigma$ of 166 N/mm^2. After $10x10^6$ cycles no cracks at all were observed and the test was stopped.

4.1.3 Test 4LA

As shown in Fig. 8 at the N side no cracks were observed. At the S side 2 cracks initiated at $0.65x10^6$ cycles at the weld toe of the flange which later joined together.

After N = 0.76×10^6 no further crack propagation was observed after the crack reached a length of 250 mm. The maximum crack depth was 17 mm.

No cracks were observed at the weld toe with the web, although at the S side the maximum measured $\Delta\sigma$ = 222 N/mm^2. Fig. 9 shows the cross sections with the cracks at the centre. The test was stopped at 1.3×10^6 cycles.

4.2 Tests with artificial defects at the weld toe with the flange

For the tests with artificial defects 3 tests have been carried out, i.e 2LA-K and 4LB-K with a load range of 1522 kN and test 3LB-K with a lower load range of 1140 kN.

4.2.1 Test 2LA-K

At the weld toe with the web the governing S side location had a measured $\Delta\sigma$ of 196 N/mm^2 but no cracks occurred. Crack initiation started at both sides from the artificial defect at the toe of the flange; first at the S side at 0.65×10^6 and then at the N side at 0.9×10^6.

At the S side cracks grew from the artificial defect along the weld toe of the flange and from there into the weld, see Fig. 10. At N = 1.45×10^6 the maximum crack length was reached and at the edges no further crack growth in depth was observed. The maximum crack depth was 16 mm.

At the N side the cracks grew from the artificial defect along the weld toe of the flange, see Fig. 10. After N = 1.45×10^6 the crack length was 28 mm and no further crack growth was observed. The maximum crack depth was 10 mm. No cracks were observed at the weld toe with the web. Fig. 11 shows the most critical cross sections at the centre over a small length; this location had the most severe cracks. The test was stopped at 2.08×10^6 cycles.

4.2.2 Test 3LB-K

At the weld toe with the web the maximum measured $\Delta\sigma$ at the N side was 166 N/mm^2. After 10x10^6 cycles no cracks in web, weld or flange were observed and the test was stopped.

4.2.3 Test 4LB-K

At the weld toe with the web the governing measured $\Delta\sigma$ at the N side was 200 N/mm^2. At the N side crack initiation started at about 0.34x10^6 at the weld toe with the web and grew along the weld toe. After N = 0.84x10^6 the maximum crack length of 250 mm was reached and at N = 1.04 x10^6 no further crack growth in depth was observed, see Fig. 12. The maximum crack depth at the N side was 17 mm.

At the S side, crack initiation started at at N = 0.76x10^6 from the artificial defect at the weld toe with the flange. After N = 1.26x10^6 the crack length at the S side was 72 mm and no further growth was observed. The maximum crack depth was 12 mm. Fig. 13 shows the most critical cross sections at the centre over a length of 72 mm. The test was stopped at 1.3x10^6 cycles.

5. Evaluation of the test results

For the evaluation of the test results initially a lower bound of the tests results for crack initiation with an assumed inverse slope of 3 is used to determine the equivalent $\Delta\sigma_2$ at 2x10^6 cycles, (see the last columns in Tables 2 and 3). The equivalent $\Delta\sigma_2$ is determined considering a conservative thickness coefficient of 0.2, see Tables 2 and 3. According to [7, 8] the recommended thickness coefficient for comparable details loaded in tension varies between 0.2 and 0.3 whereas in [5] the thickness or size effect is taken into account by relating the class for this detail loaded in tension to the flange thickness t_f plus the weld depth h_w.

In this paper, the data including a thickness correction are compared with the $\Delta\sigma$-N line for class 71 at 2x10^6 cycles for 25 mm and an inverse slope of 3 which is used in EN 1993-1-9

[5], and EN 1993-6 [6] for crane runway girders. It should be noted that IIW-XIII [7] gives a class of 80 with an inverse slope of 3 but in combination with about a 15% lower effective width. EN 13001-3-1 [9] gives for full penetration welds, depending on the quality, a class 100 or 112 also in combination with about a 15% lower effective width [1]. Both [7, 9] relate the behaviour only to $\Delta\sigma_z$ in the web.

5.1 Cracks at the weld toe with the flange

The test results with cracks at the weld toe with the flange are summarised in Table 2 and in Figs. 14 and 15.

The first observation is that the tests without artificial defects in Fig. 14 do not show significant higher results than those with artificial defects in Fig. 15, i.e. a nearly similar equivalent $\Delta\sigma_2$ = 104 N/mm^2 for test 4LA and $\Delta\sigma_2$ = 101 N/mm^2 for test 2LA-K. For end of crack growth the lower bound is governed by test 4LA with $\Delta\sigma_2$ = 110 N/mm^2.

Since the results are all within a short life range the slope of 3 cannot be confirmed with these test results but for uniform loading both EN 1993-1-9 [5] and IIW [7] also give an inverse slope of 3. Furthermore, it should be noted that tests 3LA and 3LB-K with a stress range corrected for thickness of 112 N/mm^2 sustained 10x10^6 cycles, indicating for these tests a fatigue limit for crack initiation considerably lower than 5x10^6 cycles or a shallower slope.

5.2 Cracks at the weld toe with the web or in the weld

The test results with cracks at the weld toe with the web or in the weld are presented in Table 3 and Fig. 16. The data also include a thickness correction and are again compared with the $\Delta\sigma$-N line for class 71 at 2x10^6 cycles for 25 mm From the available data there are four run outs and only 2LB and 4LB-K show crack initiations with finally a stop of crack growth.

These two tests show cracking whereas the others did not although the stress ranges were roughly in a similar band. The absence of cracks in the weld or at the weld toe with the web in tests 4LA and 2LA-K could have been influenced by some relaxation of the residual stress due to the cracks at the weld toe of the flange. A lower bound for crack initiation of the tests where cracks occurred, is given by test 4LB-K which first started cracking at the weld toe with the web, giving for an inverse slope m = 3 of the $\Delta\sigma$-N line an equivalent stress range $\Delta\sigma_2$ = 115 N/mm^2. For reaching the end of crack growth test 2LB is governing with $\Delta\sigma_2$ = 161 N/mm^2.

Here, also the results with crack initiation are limited and within a short life range which means that the slope of 3 cannot be confirmed. Further, similar as for the flange, it should be noted that tests 3LA and 3LB-K with a stress range corrected for thickness of 173 N/mm^2 sustained 10x10^6 cycles, also indicating a fatigue limit considerably lower than 5x10^6 cycles or a shallower slope.

5.3 General observations

As stated in 5.1 and 5.2, the test results are within a relatively small life span. Therefore, the stress ranges modified for thickness to 25 mm are for the number of cycles to crack initiation also directly related to the S-N line for class 71 N/mm^2 used in EN 1993-1-9 [5] and EN 1993-6 [6] for crane runway girders. The ratio between the observed stress range modified to 25 mm thickness and the S-N line for class 71 are independent from the actual slope for the test results and are shown in Tables 4 and 5.

From tables 4 and 5 it can be concluded that in all cases the ratio between the visually observed crack initiation combined with a drop in strain in the strain gauges and the S-N line for class 71 vary considerably.

This is logical and expected since this depends on local defects at the weld toes and/at the weld surface. However, in all cases crack initiation started at a $\Delta\sigma$ exceeding 1.4 times that of the class 71 S-N line. Furthermore, for the weld toe with the flange no cracks were observed for a stress range, corrected for thickness, of 112 N/mm^2, even at 10x10^6 cycles. For the weld toe with the web or the weld itself no cracks were observed for a stress range, corrected for thickness, of 173 N/mm^2, even at 10x10^6 cycles.

The maximum crack depth of a crack measured from one side of the web varies between 15 and 17 mm, thus to 50 to 60% of the web thickness.

The ratio between the number of cycles to crack initiation and that at which the crack(s) stop or reach the edge of the specimen in length and depth varies considerably. The smallest ratio is found for test 4LA with a ratio of 1.2 with only one crack at one side at the weld toe with the flange. The larger ratios from 1.5 up to 3.1 are found for specimens with cracks at both sides. In this case generally one of the cracks has either a small length or a smaller depth. This larger margin between crack initiation and end of crack growth from both sides is important because the remaining area between the cracks can locally be very small as shown in Fig. 8 for test 2LA-K.

Considering test results 3LA and 3LB-K for the weld toes at the web and flange it seems that for these line load tests under compression the fatigue limit is lower than 5x10^6 cycles and class 71 will be too low, however limited data exist.

With regard to crack growth, Van de Pas and Fischer, 1996 [10] state:

Fluctuating compressive stresses in a region of residual tensile stress will cause cracks to propagate. The cracks will stop growing after the residual stress is released or the crack

extends out of the tensile region. This agrees with the philosophy used in this investigation. They further state:

To minimize fatigue cracking at the junction of the web to the top flange the AISE Technical report No. 13 [11] requires a full penetration weld plus contoured fillet welds between the web and top flange.

However, the test results of this investigation show that crack growth will stop indeed but the cracks may be larger than expected based on the expected residual tensile stress field in the outer weld layers.

6. Summary and conclusions

6.1 Web weld toe

- Two line load tests with a stress range corrected for thickness of $\Delta\sigma$ = 173 N/mm^2) were tested to over 10x10^6 cycles without any crack initiation at all.

- Two other tests with stress ranges corrected for thickness of $\Delta\sigma$ = 231 and 204 N/mm^2 and more than 10^6 cycles only showed cracks at the weld toe with the flange and no cracks at the weld toe with the web or in the weld.

- The observed cracks in tests developed only from one side with a depth of about 50-60% of the web depth.

6.2 Flange weld toe without artificial defects

- The line load test with a stress range corrected for thickness of $\Delta\sigma$ = 112 N/mm^2 was tested to over 10x10^6 cycles without any crack initiation.

- The observed crack depths are about 15-17 mm at one side, measured perpendicular from the web side, sometimes in combination with a crack smaller in length and/or in depth at the

other side. The end of crack growth at the less critical side could have been influenced by a certain relaxation in residual stresses due to the fact that the first crack reached the full length of the specimen.

6.3 Flange weld toe with artificial defects

- The line load test with a stress range corrected for thickness of $\Delta\sigma = 112$ N/mm^2 was tested to over 10×10^6 cycles without any crack initiation.

- The tests did not show a significant difference between those without and those with artificial defects.

- The observed crack depths are about 15-17 mm measured perpendicular from the web side, sometimes in combination with a crack smaller in length and/or in depth at the other side.

6.4 Crack growth

- As expected crack growth stops after the cracks reach a certain depth, although it differs whether they grow from one side or from both sides.

- The depth of the cracks is considerably larger than initially expected. In case they grow from one side the depth will be about 50-60% of the web depth. Whereas in case they grow from both sides, which was only observed for cracks at the weld toe at the flange, the depth at one side will be about 50-60% of the web depth and at the other side the length and/or depth will be considerably smaller, although very locally the remaining cross section may be small.

- In case cracks grow only from one side the ratio between end of crack growth and crack initiation may be very small, about 1.2 whereas this ratio will be 1.5 - 3.1 for crack growth from both sides at the weld toe with the flange.

6.5 Classification

- In EN 1993-1-9 and EN 1993-6 a class 71 N/mm^2 for 2x10^6 cycles for 25 mm is given for crane runway girders with compression loading.

- Kuhlmann et al. [3] reported that based on their rolling wheel tests for welds of 6 mm with no full penetration class 92 was obtained. Wardenier et al. [1] conclude, based on the analysis of an actual crane runway girder with full penetration welds between the 75 mm flange and the 65 mm web that, corrected for thickness and assuming an inverse slope of 3, the observed crack initiation at the weld toe with the flange agrees with class 98 N/mm^2 at 2x10^6 cycles.

- Assuming an inverse slope of 3, the line load tests with full penetration welds, discussed in this paper, sustained 10x10^6 cycles with a stress range $\Delta\sigma$ of 112 N/mm^2 for the weld toes at the flange and even 173 N/mm^2 for the weld toes at the web.

- Thus, although the number of data is small, the test results for crack initiation show that class 71 N/mm^2 at 2x10^6 cycles with a fatigue limit at 5x10^6 cycles in EN 1993-1-9 and EN 1993-6 for crane runway girders seems to be too conservative for multi-layered full penetration welds loaded in compression. The more, because the comparison given is for crack initiation in the tests and not for failure.

7. References

[1] Wardenier, J. Vries, P.A. de. Timmerman, G. Evaluation of cracks in an offshore crane runway girder - I. Submitted for publication in Steel Construction, Issue 4; Nov. 2016.

[2] Wardenier, J. Vries, P.A. de. Timmerman, G. Fatigue behaviour under a concentrated wheel compression loading. Unpublished results, to be published.

[3] Kuhlmann, U. Herter, K-H. Euler, M. Retteneier, P. Weihe, S. Versuchsbasierte Ermüdungsfestigkeit von Konstruktionsdetails mit Radlasteinleitung. Stahlbau 84, Heft 9, 2015.

[4] Euler, M. Kuhlmann, U. Fatigue evaluation of crane rail welds using local concepts. International Journal of Fatigue, 33, Elsevier; 2011, pp. 111-1126.

[5] EN 1993-1-9. Design of steel structures. Fatigue. CEN, Brussels, Belgium, 2006.

[6] EN 1993-6. Design of steel structures. Crane supporting structures. CEN, Brussels, Belgium, 2007.

[7] Hobbacher, A. Recommendations for fatigue design of welded joints and components. Revision of IIW Doc. XIII 2151r4-07. IIW Doc. XV-1440-13, IIW, Paris, France, 2013.

[8] DNV. Fatigue design of offshore steel structures. Recommended Practice DNV-RP-C203. Norway, 2010.

[9] EN-13001-3-1 Cranes - General design-Part 3-1. Limit states and proof of competence of steel structures. CEN, Brussels, Belgium, 2013.

[10] Pas, J.van de. Fisher, J.M. Crane girder design. Paper presented at the 1996 National Steel Construction Conference. Modern Steel Construction, Phoenix, Arizon, USA, 1096: pp. 48 – 57.

[11] AISE. Technical report No. 13. Guide for design and Construction of Mill Buildings, Pittsburgh, PA, USA, 1991.

Abbreviations used

DNV: Det Norske Veritas

IIW: International Institute of Welding

AISE: Association of Iron and Steel Engineers

List of Tables

Table 1 Dimensions, steel grades and qualities of the line load test specimens

Table 2 Test results for Line loading - cracks at the weld toe with the flange

Table 3 Test results for Line loading - cracks at the weld toe with the web or in the weld

Table 4 Test results for crack initiation at the weld toe with the flange related to class 71 curve in EN 1993-1-9 [5] and EN 1993-6 [6]

Table 5 Test results for crack initiation in or at the weld toe with the web related to class 71 curve in EN 1993-1-9 [5] and EN 1993-6 [6]

Table 1 Dimensions, steel grades and qualities of the line load test specimens

	Dimension mm	**Steel grade/quality**	**actual f_y** N/mm^2	**actual f_u** N/mm^2
rail, top & bottom	185x35	DILLIDUR 400V	792	925
flange top & bottom	300x35**	S460G2+M-Z35	484	550
web	450x30	EH36	415*	550*

* average value ** machined from 40 to 35 mm

Tables 2 and 3, see next pages

Table 4 Test results for crack initiation at the weld toe with the flange related to class 71 curve in EN 1993-1-9 [5] and EN 1993-6 [6]

Line loading - weld toe flange					
test	$\Delta\sigma_i$	N_i	$\Delta\sigma_i$	$\Delta\sigma$	
	average	initiation	$(t/25)^{0.2}$	71 curve	ratio
	N/mm^2	x10^6	N/mm^2	N/mm^2	
2LB	151	0.9	161	93	1.73
4LA	143	0.65	151	103	1.47
2LA-K	137	0.65	146	103	1.42
4LB-K	143	0.76	152	98	1.55

Table 5 Test results for crack initiation in or at the weld toe with the web related to class 71 curve in EN 1993-1-9 [5] and EN 1993-6 [6]

Line loading - weld toe web or weld					
test	$\Delta\sigma_i$	N_i	$\Delta\sigma_i$	$\Delta\sigma$	
	measured	initiation	$(t/25)^{0.2}$	71 curve	ratio
	N/mm^2	x10^6	N/mm^2	N/mm^2	
2LB	174	0.90	181	93	1.95
4LB-K	200	0.34	208	128	1.62

Table 2 Test results for Line loading - cracks at the weld toe with the flange

Line loading - weld toe flange										$\Delta\sigma$ values for 25 mm		
test	load ΔF	t_{flange}	t_w+2b_w	$\Delta\sigma_i$	N_i	N	N	max. crack size		$\Delta\sigma_i$	$\Delta\sigma_2$	$\Delta\sigma_2$
				average	initiation	stop	end test	length	depth	$(t/25)^{0.2}$	crack init.	max. crack
	kN	mm	mm	N/mm^2	x10^6	x10^6	x10^6	mm	mm	N/mm^2	N/mm^2	N/mm^2
2LB	1522	34.0	40.3	151	0.90	1.40	2.08	S250/N135	S15	161	123	143
3LA*)	1140	34.1	43.5	105	>10,0	>10,0	10	0	0	112	>>112	>>112
4LA	1522	33.0	42.5	143	0.65	0.76	1.3	250	**S17**	151	**104**	**110**
2LA-K	1522	34.4	44.3	137	0.65	1.45	2.08	S250/N28	S16+N10	146	**101**	132
3LB-K*)	1140	35.0	43.5	105	>10,0	>10,0	10	0	0	112	>>112	>>112
4LB-K	1522	33.8	42.5	143	0.76	1.26	1.3	72	S12	152	110	130

*) No cracks

Table 3 Test results for Line loading - cracks at the weld toe with the web or in the weld

Line loading - weld toe web or weld										$\Delta\sigma$ values for 25 mm		
test	load ΔF	t_w		$\Delta\sigma_i$	N_i	N	N	max. crack size		$\Delta\sigma_i$	$\Delta\sigma_2$	$\Delta\sigma_2$
			average	measured	initiation	stop	end test	length	depth	$(t/25)^{0,2}$	crack init.	max. crack
	kN	mm	N/mm^2	N/mm^2	x10^6	x10^6	x10^6	mm	mm	N/mm^2	N/mm^2	N/mm^2
2LB	1522	30.3	201	174	0.90	1.40	2.08	250	S-15	181	139	161
3LA*)	1140	30.5	150	166	>10	-	10	0	0	173	>173	>173
4LA*)	1522	30.5	200	222	-	-	1.3	0	0	231	>231	>231
2LA-K*)	1522	30.3	201	196	-	-	2.08	0	0	204	>204	>204
3LB-K*)	1140	30.5	150	166	>10	-	10	0	0	173	>173	>173
4LB-K	1522	30.5	200	200	0.34	1.04	1.3	250	N-17	208	115	167

*) No cracks

List of Figures

Fig. 1. Normal stress σ_z and local shear stress τ_{xz} due to wheel load [3, 4]

Fig. 2. I-beam test specimen for variable line loading; approximate scale thicknesses 1 : 2

Fig. 3. Artificial elliptical defect (under 10°) by the electrical discharge machining method

Fig. 4. Test rig with I-beam specimen for wheel load tests

Fig. 5. Welds and strain gauge locations at the centre of the web

Fig. 6. Cracks in test 2LB

Fig. 7.Cross section of the cracks at the centre of the test specimen 2LB

Fig. 8. Cracks in test 4LA

Fig. 9. Cross section of the cracks at the centre of the test specimen 4LA

Fig. 10. Cracks in slices, test 2LA-K

Fig. 11. Cross section of the cracks at the centre of the test specimen 2LA-K

Fig. 12. Cracks in test 4LB-K

Fig. 13. Cross section of the cracks at the centre of the test specimen 4LB-K

Fig. 14. Test results 2LB, 3LA and 4LA corrected for thickness for the flange weld toe compared with the basic $\Delta\sigma$-N line of EN 1993-1-9 for 25 mm (class 71 at $2x10^6$)

Fig. 15. Test results 2LA-K, 3LB-K and 4LB-K corrected for thickness for the flange weld toe compared with the basic $\Delta\sigma$-N line of EN 1993-1-9 for 25 mm (class 71 at $2x10^6$)

Fig. 16. Test results 2LB, 3LA, 4LA, 2LA- K, 3LB-K and 4LB-K, corrected for thickness for the web weld toe compared with the basic $\Delta\sigma$-N line of EN 1993-1-9 for 25 mm (class 71 at $2x10^6$)

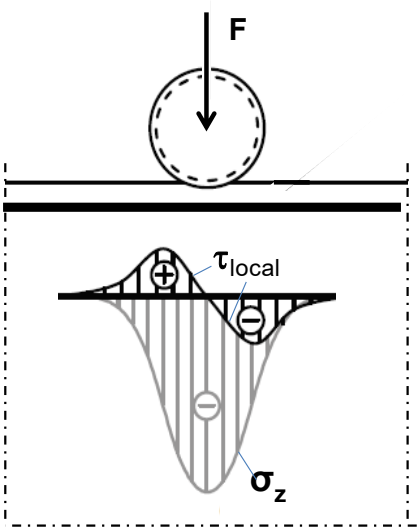


Fig. 1. Normal stress σ_z and local shear stressτ_{xz} due to wheel load [3, 4]

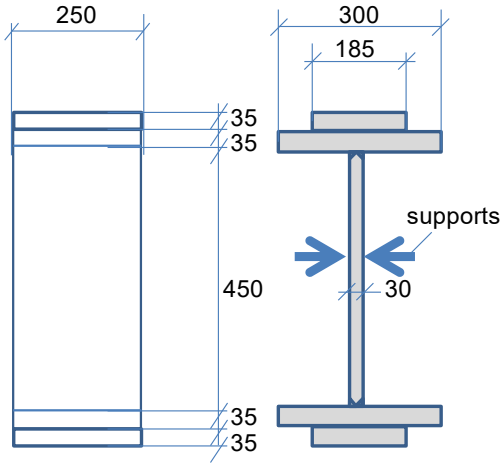


Fig. 2. I-beam test specimen for variable line loading; approximate scale thicknesses 1 : 2



Fig. 3. Artificial elliptical defect (under 10°) by the electrical discharge machining method

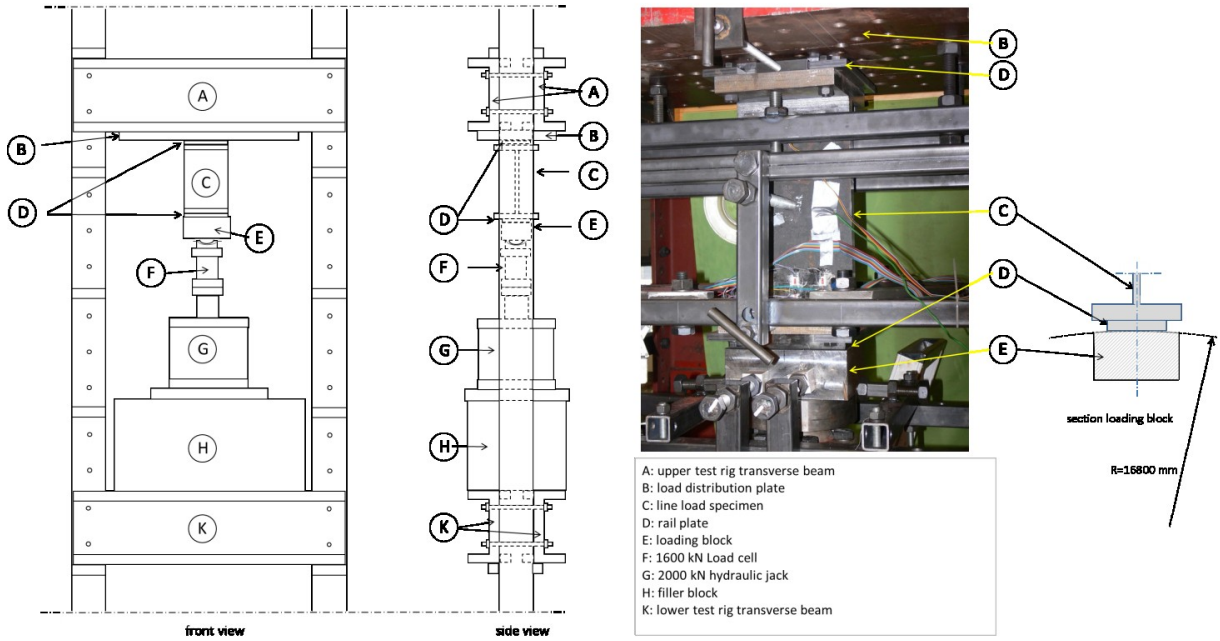


Fig. 4. Test rig with I-beam specimen for line load tests

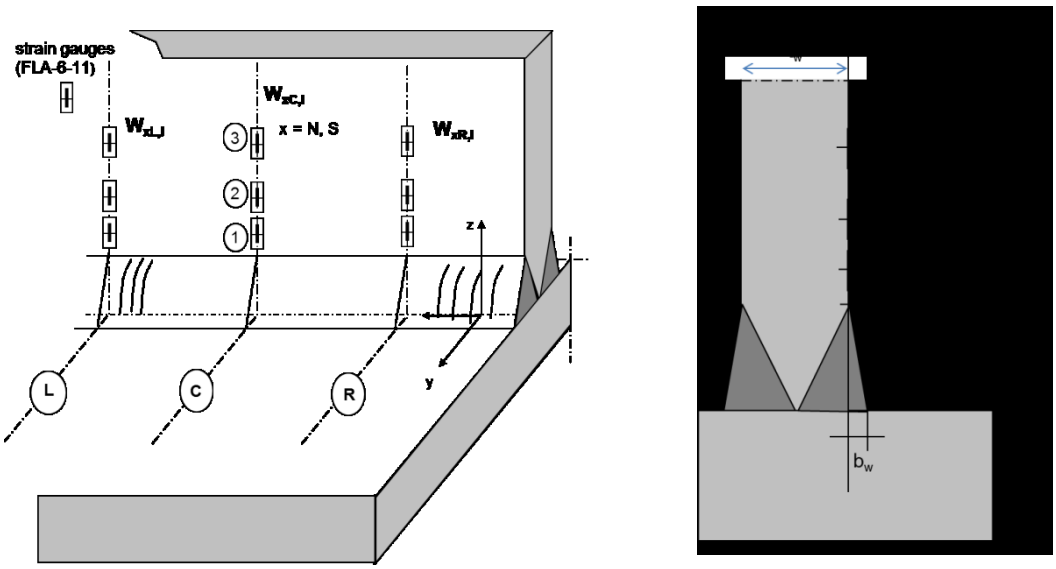
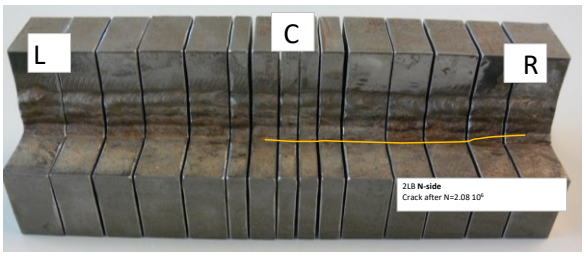
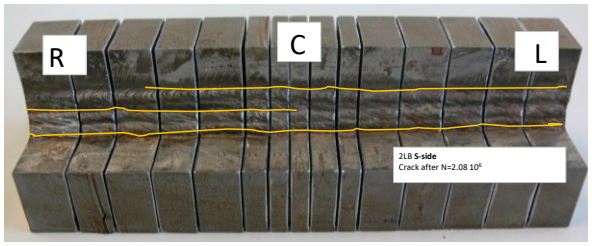


Fig. 5. Welds and strain gauge locations



N-side



S-side

Fig. 6. Cracks in test 2LB

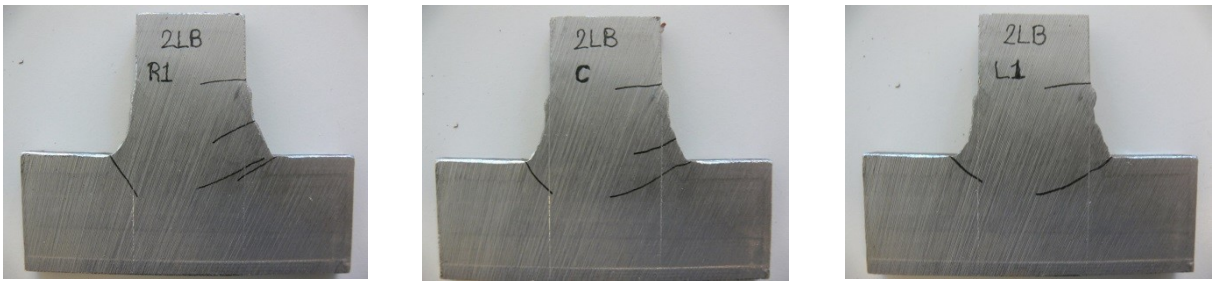
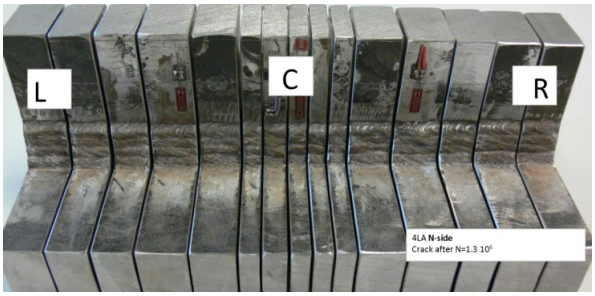
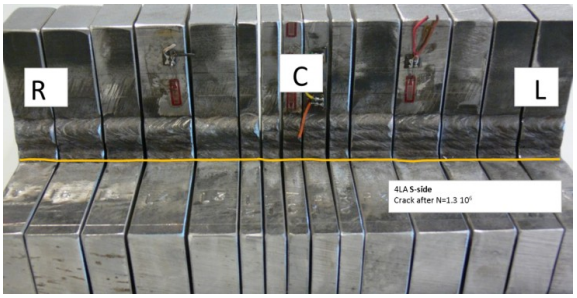


Fig. 7.Cross section of the cracks at the centre of the test specimen 2LB



N-side

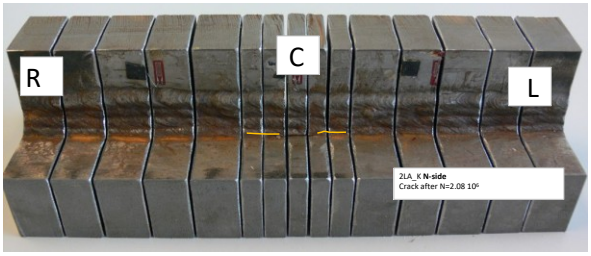


S-side

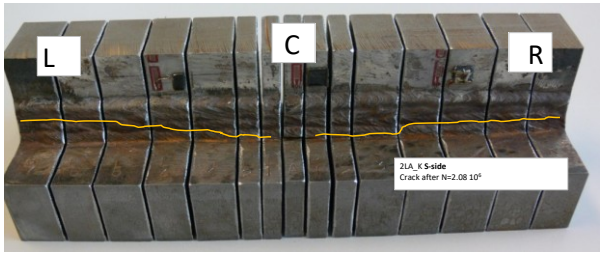
Fig. 8. Cracks in test 4LA



Fig. 9. Cross section of the cracks at the centre of the test specimen 4LA

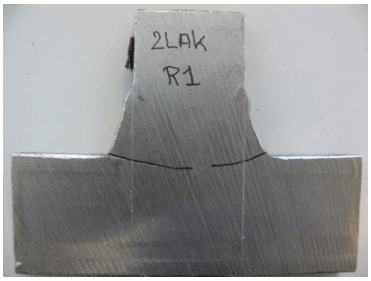


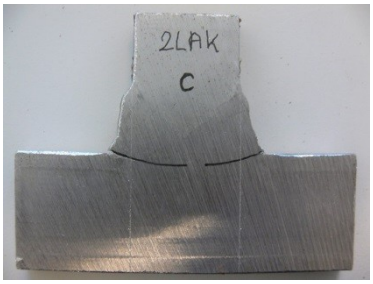
N-side



S-side

Fig. 10. Cracks in slices, test 2LA-K





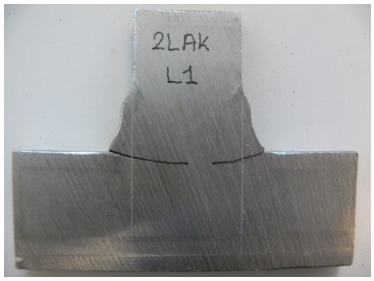
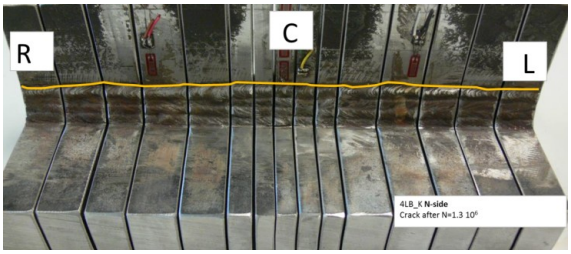
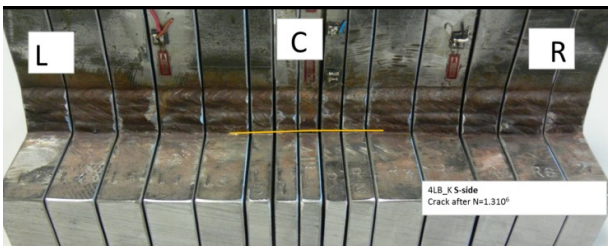


Fig. 11. Cross section of the cracks at the centre of the test specimen 2LA-K



N-side



S-side

Fig. 12. Cracks in test 4LB-K





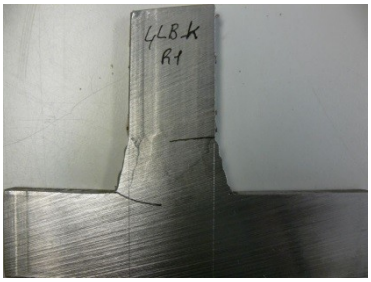


Fig. 13. Cross section of the cracks at the centre of the test specimen 4LB-K

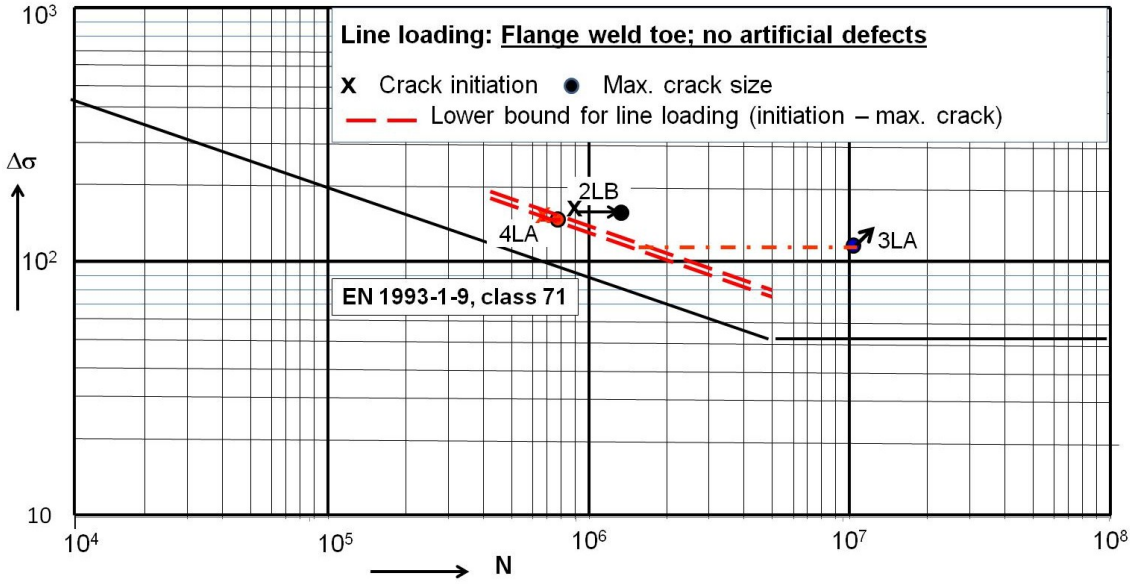


Fig. 14. Test results 2LB, 3LA and 4LA corrected for thickness for the flange weld toe compared with the basic Δσ-N line of EN 1993-1-9 for 25 mm (class 71 at $2x10^6$)

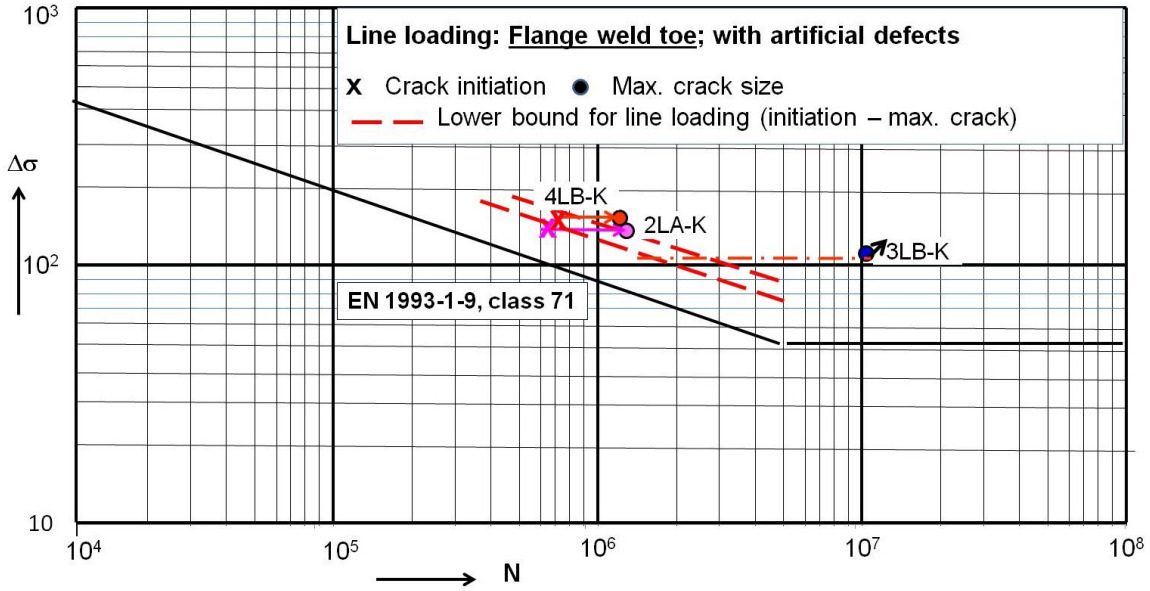


Fig. 15. Test results 2LA-K, 3LB-K and 4LB-K corrected for thickness for the flange weld toe compared with the basic Δσ-N line of EN 1993-1-9 for 25 mm (class 71 at $2x10^6$)

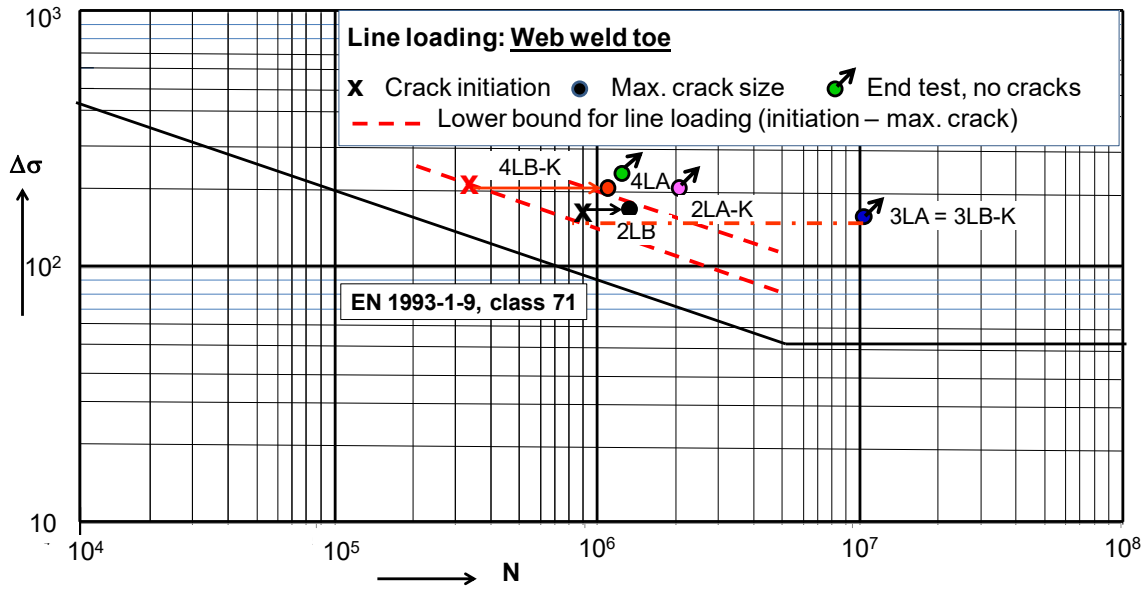


Fig. 16. Test results 2LB, 3LA, 4LA, 2LA- K, 3LB-K and 4LB-K, corrected for thickness for the web weld toe compared with the basic Δσ-N line of EN 1993-1-9 for 25 mm (class 71 at $2x10^6$)

Authors:

Prof. dr. ir. Jaap Wardenier, j.wardenier@tudelft.nl, Corresponding Author
Faculty of Civil Engineering and Geosciences, Delft University of Technology,

P.O.Box 5048, 2600GA Delft, The Netherlands and

Centre for Offshore Research & Engineering and Department of Civil & Environmental Engineering, National University of Singapore,

#E1A-07-03, 1 Engineering Drive 2, Kent Ridge, Singapore 117576

Ir. Peter de Vries, P.A.deVries@tudelft.nl

Faculty of Civil Engineering and Geosciences, Delft University of Technology,

P.O.Box 5048, 2600GA Delft, The Netherlands

Ir. Gerrit Timmerman, GTIMMERMAN@PT-STRUCTURAL.COM

PT Structural Design & Analysis B.V.

Boelewerf 22, 2987 VD Ridderkerk